



Neutron–gamma discrimination based on pulse shape discrimination in a Ce:LiCaAlF₆ scintillator

Atsushi Yamazaki^{a,*}, Kenichi Watanabe^a, Akira Uritani^a, Tetsuo Iguchi^b, Noriaki Kawaguchi^c, Takayuki Yanagida^d, Yutaka Fujimoto^d, Yuui Yokota^d, Kei Kamada^d, Kentaro Fukuda^c, Toshihisa Suyama^c, Akira Yoshikawa^{d,e}

^a Department of Materials, Physics and Energy Engineering, Graduate School of Engineering, Nagoya University, Japan

^b Department of Quantum Engineering, Graduate School of Engineering, Nagoya University, Japan

^c Tokuyama Corporation, Japan

^d Institute of Multidisciplinary Research for Advanced Materials (IMRAM), Tohoku University, Japan

^e New Industry Creation Hatchery Center (NICHe), Tohoku University, Japan

ARTICLE INFO

Available online 24 February 2011

Keywords:

Neutron detection

Neutron scintillator

Pulse shape discrimination

Neutron/gamma discrimination

ABSTRACT

We demonstrate neutron–gamma discrimination based on a pulse shape discrimination method in a Ce:LiCAF scintillator. We have tried neutron–gamma discrimination using a difference in the pulse shape or the decay time of the scintillation light pulse. The decay time is converted into the rise time through an integrating circuit. A ²⁵²Cf enclosed in a polyethylene container is used as the source of thermal neutrons and prompt gamma-rays. Obvious separation of neutron and gamma-ray events is achieved using the information of the rise time of the scintillation light pulse. In the separated neutron spectrum, the gamma-ray events are effectively suppressed with little loss of neutron events. The pulse shape discrimination is confirmed to be useful to detect neutrons with the Ce:LiCAF scintillator under an intense high-energy gamma-ray condition.

© 2011 Elsevier B.V. All rights reserved.

1. Introduction

Neutron detection techniques play an important role in various fields. As one of the promising candidates of neutron detectors with high efficiency, rare-earth-ion-doped LiCaAlF₆ (LiCAF) scintillators have been developed [1–5]. The LiCAF scintillator contains lithium-6 with a large neutron absorption cross-section and has low gamma-ray sensitivity due to its light composition. Moreover, large single crystal growing is possible with the Czochralski technique. Since a ⁶Li(*n*, α) reaction has a relatively large Q-value of 4.8 MeV, the scintillation light yield caused by neutron reactions is higher than that caused by gamma-rays or fast electrons in spite of low conversion efficiency from deposited energy to scintillation photons for heavy charged particles. We, therefore, can discriminate neutron events from gamma-ray events by the pulse height discrimination [6–8]. We, however, must consider the influence of gamma-rays when using a large crystal to increase the detection efficiency for neutrons. When detecting epi-thermal neutrons, for which the neutron absorption cross-section of ⁶Li is low, we should use a large crystal to keep high detection efficiency. Usually neutron fields are also intense gamma-ray fields. Especially, when a neutron is

absorbed by a nucleus a prompt gamma ray, which frequently has relatively high energy, is emitted. In intense high-energy gamma-ray yields, the neutron/gamma discrimination, only by the pulse height discrimination, is inadequate. Therefore, the neutron/gamma discrimination method other than the pulse height discrimination is also necessary especially in epi-thermal neutron measurements.

We propose to apply the pulse shape discrimination, which is frequently used in organic liquid scintillators, to selectively detect neutrons with the Ce:LiCAF scintillator. In this paper, we demonstrate the neutron–gamma discrimination using the pulse shape discrimination in the Ce:LiCAF scintillator.

2. Experimental setup

An experimental setup is shown in Fig. 1. A ²⁵²Cf enclosed in a polyethylene moderator was used as a source of thermal neutrons and prompt gamma-rays. The Ce:LiCAF crystal with a size of 10 × 10 × 1 mm³ was mounted on a photomultiplier tube (PMT, H6612, Hamamatsu) with optical grease. The Ce:LiCAF scintillator was covered by Teflon tapes to collect the scintillation photons. Furthermore, the scintillator and the PMT were covered with an aluminum foil to shield ambient lights. The applied voltage of the PMT was –1700 V. The Ce:LiCAF scintillator unit was surrounded by LiF plates except for the surface facing the neutron source in order to

* Corresponding author.

E-mail address: a-yamazaki@nucl.nagoya-u.ac.jp (A. Yamazaki).

suppress scattered neutrons to come. The output signal from the PMT was read out by a charge-sensitive preamplifier (model 113, ORTEC) and sent to a shaping amplifier (model 571, ORTEC). Here,

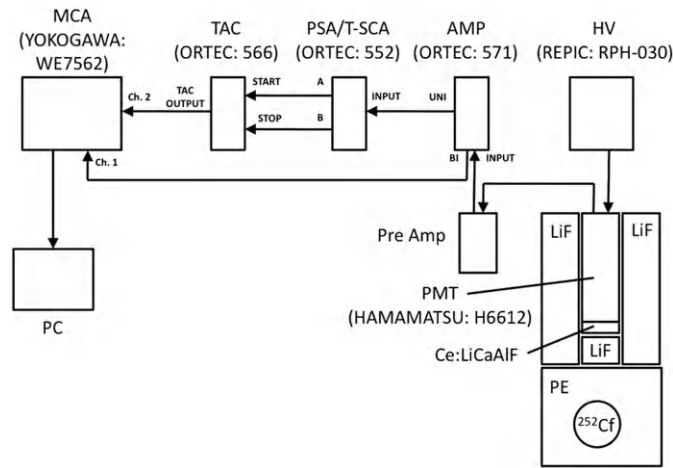


Fig. 1. Experimental setup.

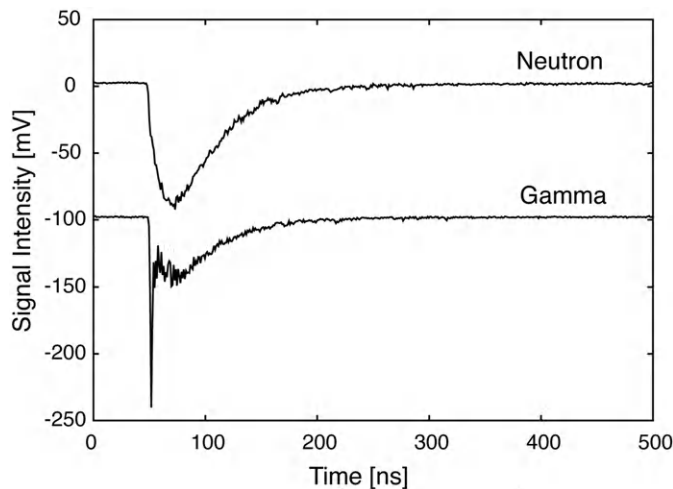


Fig. 2. Typical scintillator pulse for neutron and gamma-ray induced events.

the charge signal from the PMT was integrated. The output signal of the shaping amplifier was divided into two signal processing circuits, which are the pulse height and the rise time analysis circuits. For the pulse height analysis, one of the signals was sent to one of the inputs of a dual multi channel analyzer (Dual MCAs, WE7562, Yokogawa), which can record a time stamp. The other signal was sent into a pulse shape analyzer (PSA/T-SCA, model 552, ORTEC), which generates two timing signals of 0.1 and 0.9 fractions of the signal rising, the two signals were fed into the timing-to-amplitude converter (TAC, model 566, ORTEC), which converts the time differences between two input signals into the pulse amplitude. The time difference of these signal represents the rise time of the signal pulses. The output signal of the TAC was also sent into the residual input of the dual MCA. The pulse height and the rise time were recorded through the dual MCA into a PC. Coincident events between the pulse height signals and the rise time signals were picked up.

3. Experimental results of neutron–gamma discrimination

Typical scintillator pulses induced by neutrons and gamma-rays are shown in Fig. 2. The scintillator pulses induced by gamma-rays have the rapid luminescence component. Fig. 3 shows the two-dimensional histogram between the pulse height and the rise time signals. Since the scintillation signals obtained by the photomultiplier were integrated, the decay time of the scintillation was derived from the rise time of the integrated signals. In the case of Fig. 3(a), the Ce:LiCAF scintillator was irradiated by neutrons from the ²⁵²Cf source without a LiF neutron shielding plate between the neutron source and the Ce:LiCAF scintillator, in other words, the scintillator was directly irradiated by the neutrons from ²⁵²Cf source. We confirmed that the obvious spot caused by neutron incidents was clearly recognized. In the case of Fig. 3(b), the LiF neutron shielding plate of 30 mm thickness was inserted between the scintillator and the neutron source. By shielding neutrons, a weak neutron field with relatively intense gamma-ray backgrounds was imitated. We confirmed that the neutron and the gamma-ray events were obviously separated. The dashed line represents the threshold rise time for discriminating the neutron and gamma-ray events. This line is determined as the lower edge of the neutron peak in the rise time spectrum. Discussion on the threshold rise time will be done later in detail. Fig. 4 shows pulse height spectra separated

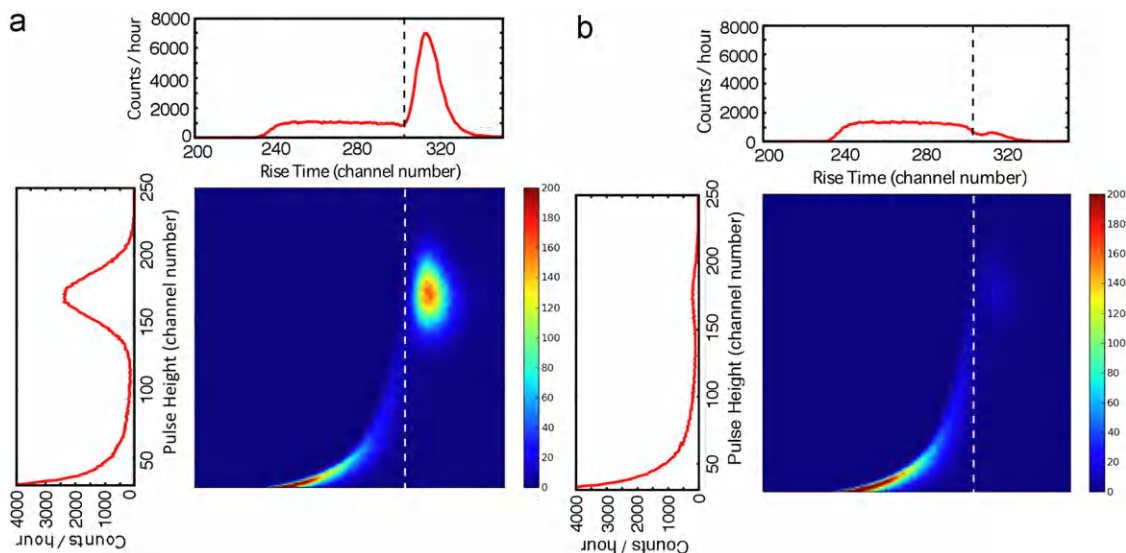


Fig. 3. Two-dimensional plot of pulse height versus rise time in scintillation signals. (a) Without LiF plate for shielding the neutrons and (b) with LiF plate for shielding the neutrons.

by the rise time of the scintillation. Fig. 4(a) is total pulse height spectrum obtained from the Ce:LiCAF scintillator irradiated by the neutrons and the gamma-rays. Fig. 4(b) and (c) shows the pulse

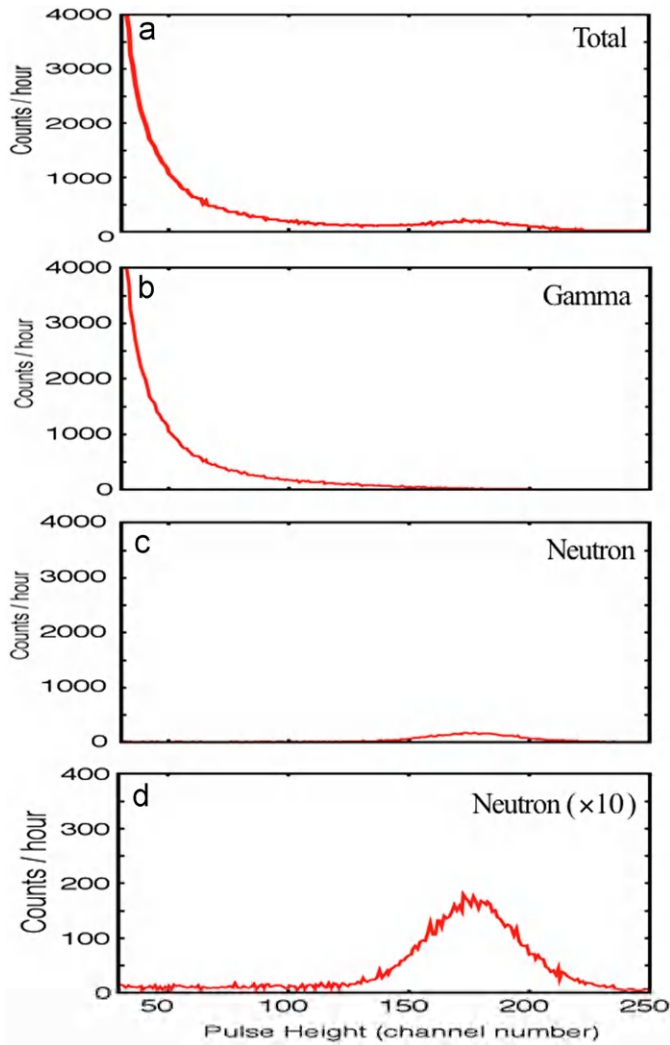


Fig. 4. Pulse shape discrimination using the rise time. (a) Total pulse height spectra, (b) pulse height spectra of gamma-rays separated by the pulse shape discrimination using the rise time, (c) pulse height spectra of neutrons separated by the pulse shape discrimination using the rise time, and (d) pulse height spectra magnified by factor of 10 in the y direction compared to (c).

height spectra for signals having the shorter and longer rise time than the threshold one, respectively. Fig. 4(b) and (c) consequently represents pulse height spectra induced by gamma-rays and the neutrons, respectively. Fig. 4(d) was vertically expanded by a factor of ten. In this spectrum, only the neutron events were observed and the gamma-ray events were effectively suppressed without loss of the neutron events. Through these basic experiments, we concluded that the pulse shape discrimination was useful to suppress the gamma-ray events especially in the large Ce:LiCAF crystal.

We assessed the gamma-ray rejection property. The gamma-ray rejection property depends on the rise time threshold level. The events induced by neutrons produce the thermal neutron peak in the pulse height spectrum. The region of interest (ROI) in the pulse height spectrum, therefore, should be set at the region of the thermal peak. The region of thermal neutron peak is set to higher pulse height region than the pulse height of the thermal peak position minus 2σ . Because our targets are neutron events, the ROI in the two-dimensional histogram like that in Fig. 3 should be set to higher region than a given rise time threshold. In this ROI, we estimated the relative neutron and gamma-ray

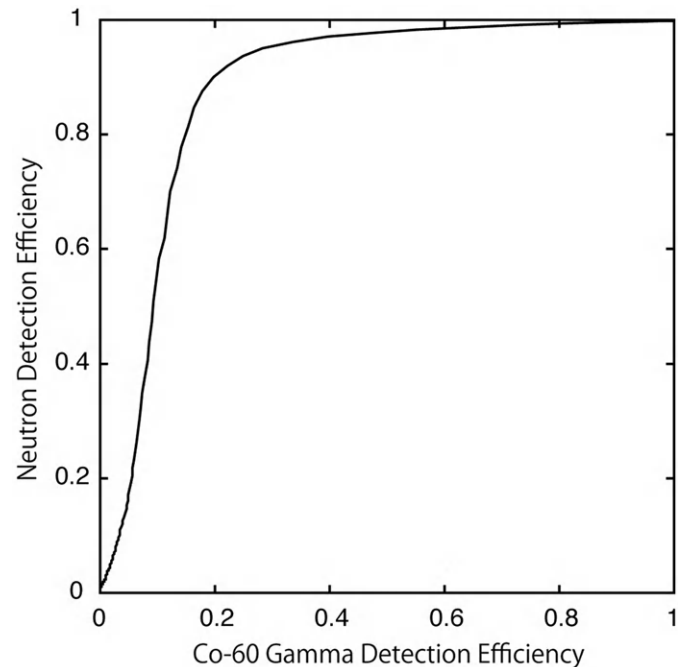


Fig. 6. Relationship between neutron and gamma-ray relative detection efficiency.

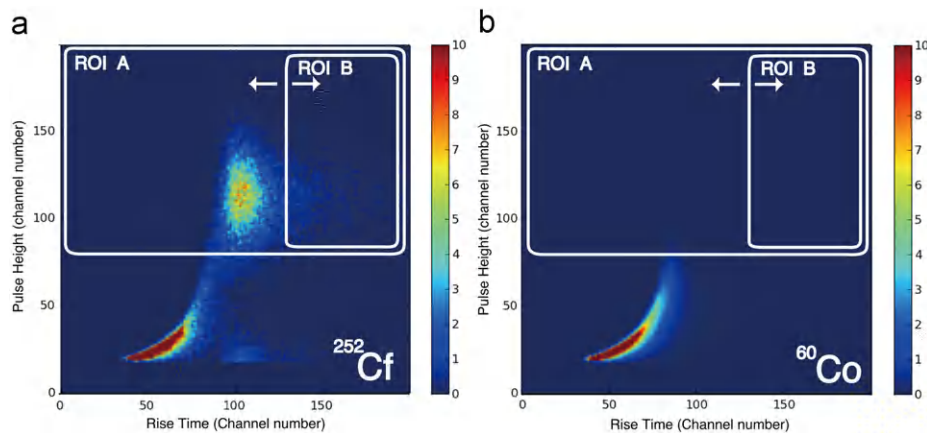


Fig. 5. ROI with the rise time discrimination (ROI-B) and ROI without rise time discrimination (ROI-A) in the two-dimensional histogram obtained by neutron and gamma-ray irradiation, respectively. (a) ^{252}Cf source and (b) ^{60}Co source.

detection efficiency. The ^{252}Cf neutron source and ^{60}Co gamma-ray source were used for estimation of the neutron and gamma-ray detection efficiency, respectively. Fig. 5(a) and (b) shows the ROI with the rise time discrimination (ROI-B) and ROI without rise time discrimination (ROI-A) in the two-dimensional histogram obtained by neutron and gamma-ray irradiation, respectively. The counts in the ROI-A and B represent the counts obtained with and without the rise time discrimination. The relative detection efficiency was determined as the ratio of the event count in the ROI-B to the one in the ROI-A. Fig. 6 shows the relationship between neutron and gamma-ray relative detection efficiency. This curve is determined by changing the threshold rise time. From Fig. 6, when the relative detection efficiency for neutrons is 90%, we can remove the 80% gamma-ray event.

4. Conclusions

When detecting epi-thermal neutrons with an inorganic scintillator, for which the absorption cross-section is low, we should use a large crystal to keep high detection efficiency. The influence of gamma-rays becomes a problem when a large crystal is used to increase the detection efficiency for neutrons, since usual neutron fields are also intense gamma-ray fields.

We therefore conducted an experiment of the neutron–gamma discrimination based on the pulse shape discrimination method in the Ce:LiCAF scintillator. As a result, obvious separation of neutron

and gamma-ray events is confirmed using the information of the rise time of the scintillation light pulse. In the separated neutron spectrum, the gamma-ray events are effectively suppressed with little loss of neutron events. The pulse shape discrimination was confirmed to be useful to detect neutrons with the Ce:LiCAF scintillator under an intense high-energy gamma-ray field.

References

- [1] N. Kawaguchi, T. Yanagida, A. Novoselov, K.J. Kim, K. Fukuda, A. Yoshikawa, M. Miyake, M. Baba, Neutron responses of Eu^{2+} activated LiCaAlF_6 scintillator, in: Proceedings of the Nuclear Science Symposium Conference Record, IEEE NSS/MIC, (2008), 1174–1176.
- [2] A. Yoshikawa, T. Yanagida, K.J. Kim, N. Kawaguchi, S. Ishizu, K. Fukuda, T. Suyama, M. Nikl, M. Miyake, M. Baba, Crystal growth, optical properties and neutron responses of Ce^{3+} doped LiCaAlF_6 single crystal, in: Proceedings of the Nuclear Science Symposium Conference Record, IEEE NSS/MIC, IEEE Dresden (2008), 1212–1214.
- [3] A. Yoshikawa, T. Yanagida, Y. Yokota, N. Kawaguchi, S. Ishizu, K. Fukuda, T. Suyama, K.J. Kim, J. Pejchal, M. Nikl, K. Watanabe, M. Miyake, M. Baba, K. Kamada, IEEE Trans. Nucl. Sci. NS-56 (Issue 6, Part 2) (2009) 3796.
- [4] N. Kawaguchi, T. Yanagida, Y. Yokota, K. Watanabe, K. Kamada, K. Fukuda, T. Suyama, A. Yoshikawa, Neutron responses of Eu^{2+} activated LiCaAlF_6 scintillator, in: Proceedings of the Nuclear Science Symposium Conference Record, IEEE NSS/MIC, (2009), 1493–1495.
- [5] T. Yanagida, A. Yoshikawa, Y. Yokota, S. Maeo, N. Kawaguchi, S. Ishizu, K. Fukuda, T. Suyama, Opt. Mater. 32 (2009) 311.
- [6] R.J. Ginther, J.H. Schulman, IRE Trans. Nucl. Sci. NS-5 (1958) 92.
- [7] A.R. Spowart, Nucl. Instr. and Meth. 135 (1976) 441.
- [8] A.R. Spowart, Nucl. Instr. and Meth. 135 (1977) 19.